Ligand-Induced Changes in the *Streptomyces lividans* TipAL Protein Imply an Alternative Mechanism of Transcriptional Activation for MerR-Like Proteins†

Mark L. Chiu,‡ Patrick H. Viollier, Takaaki Katoh,§ Jeremy J. Ramsden,|| and Charles J. Thompson*,||

Biozentrum, University of Basel, Klingelbergstrasse 70, CH-4056 Basel, Switzerland

Received February 15, 2001; Revised Manuscript Received August 7, 2001

ABSTRACT: TipAL is a *Streptomyces* transcriptional activator assigned to the MerR/SoxR family based both on homology within its putative DNA recognition domain and the fact that its operator binding sites lie within a region of its promoter normally occupied by RNA polymerase. The *tipA* gene is also independently translated as the C-terminal ligand-binding domain of TipAL (TipAS; residues 111−254). Both TipAS and TipAL share broad recognition specificity for cyclic thiopeptide antibiotics. The molecular mechanism by which TipAL catalyzes prokaryotic transcriptional activation at the *tipA* promoter (*ptipA*) in response to thiostrepton was studied using a combination of analytical ultracentrifugation (AU), circular dichroism (CD), optical waveguide lightmode spectroscopy (OWLS; a sensitive in situ binding assay), and mutational analyses. AU showed that TipAL, but not TipAS, was a dimer in solution in the presence or absence of thiostrepton. This indicated that activation of TipAL by thiostrepton was not mediated by changes in multimerization and mapped the dimerization domain to its N-terminal 110 amino acids, presumably within amino acids predicted to form a coil-coil domain (residues 77−109). CD spectra showed that TipAL had more α-helical content than TipAS, probably because of the presence of the additional N-terminal region. The helicity of TipAL and TipAS both increased slightly after binding thiostrepton demonstrating conformation changes upon thiostrepton binding. OWLS experiments determined the overall binding constants via measurements of association and dissociation rates for both TipA proteins and RNA polymerase with *ptipA*. Thiostrepton slightly enhanced the rate of specific association of TipAL with *ptipA*, but drastically lowered the rate of dissociation from the binding site. TipAL-thiostrepton increased the affinity of RNA polymerase for *ptipA* more than 10-fold. In conjunction with genetic experiments, we propose that, while there are some similarities, the mechanism by which TipAL activates transcription is distinctly different from the established MerR/SoxR paradigm.

TipAL is a transcriptional regulator that reacts with diverse cyclic peptide antibiotics and thereby activates gene expression in different *Streptomyces* strains. It has been studied most extensively in *Streptomyces lividans* where the antibiotic thiostrepton induces accumulation of thiostrepton-induced proteins (Tip) and resistance to several structurally heterogeneous antibiotics (*1*). Two of these proteins, TipAL and TipAS, are alternative in-frame translational products of the same gene (*tipA*, Figure 1). TipAL is needed for thiostrepton-induced transcription of its promoter [*ptipA* (*2*)] both in vivo (*2*) and in vitro (*3*). The TipAL binding-site is an inverted repeat sequence (Figure 2), mapped by DNase footprinting to nucleotides located −13 to −36 bp upstream of the transcriptional start site (*3*). This binding-site is within the region of the promoter normally occupied by RNA polymerase (RNAP),[1] between the putative −10 and −35 recognition hexamers. In vitro studies have shown that transcriptional activation is enhanced (*3*) by a covalent interaction between thiostrepton and TipAL (*4*).

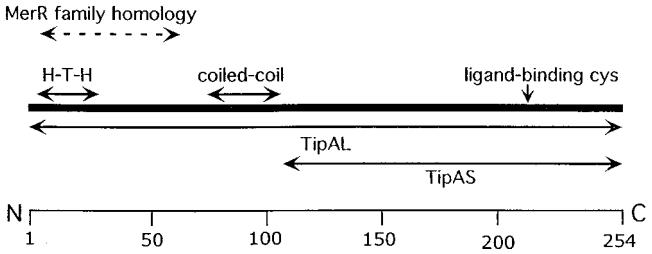

FIGURE 1: Primary structure of TipAS and TipAL proteins. Both TipAS and TipAL share a carboxyl-terminus containing a cysteine residue that binds covalently to thiostrepton-like thiopeptide antibiotics (*2*). TipAL has sequence similarity to other transcriptional regulators of the MerR family that share with it a putative N-terminal helix-turn-helix (H-T-H) motif and a predicted coiled-coil domain (*35*, *45*).

† This work was partially funded by the Swiss National Science Foundation Grant NF3100-039669.

* To whom correspondence should be addressed. Fax: + 41 61 267 2118. Phone: + 41 61 267 2116. E-mail: charles-j.thompson@unibas.ch.

‡ Present address: Department of Chemistry and Biochemistry, McNulty Hall, Seton Hall University, 400 South Orange Street, South Orange, NJ 07079.

§ Shionogi Research Laboratories, Shionogi & Co., Ltd., 12-4, Sagisu 5 chome, Fukushima-ku, Osaka 553-0002, Japan.

|| These authors contributed equally to this work.

[1] Abbreviations: AU, analytical ultracentrifugation; bp, base pairs; c_b, bulk concentration; CD, circular dichroism; EDTA, ethylenediaminetetraacetic acid; k_a association rate coefficient; k_B, Boltzmann constant; k_d, dissociation rate coefficient; KT, *Streptomyces lividans 1326* containing a disrupted *tipAL* gene; M_r, molecular mass; N_a, Avogadro's number; OWLS, optical waveguide lightmode spectroscopy; PAGE, polyacrylamide gel electrophoresis; *ptipA*, the promoter of the *tipA* gene; *R*, gas constant; RNAP, RNA polymerase; TPP, tetraphenylphosphonium chloride; SDS, sodium dodecyl sulfate; SE, sedimentation equilibrium; SV, sedimentation velocity.

10.1021/bi010328k CCC: $20.00
Published on Web 10/05/2001

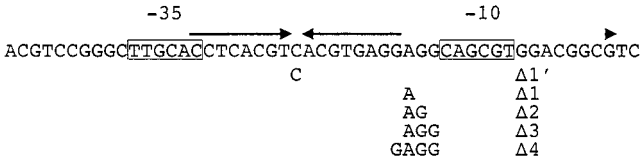

FIGURE 2: Genetic studies of the *ptipA* promoter sequence. Oligonucleotide primers A (AACTGAAGCTTACGTCCGGGCTTGCACCTCA) and B (AACTGGAATTCGACGCCGTCCACGCTGCCTC) were used to amplify a 51-bp fragment from pAK108 (*1*) including putative −10 and −35 RNAP recognition hexamers (boxed), TipAL binding sites (inverted repeat indicated by arrows) and transcriptional start site (arrowhead) defining a reduced *tipA* promoter sequence of 51 bp. This fragment was cleaved at its termini with *Hin*dIII and *Eco*RI termini, subcloned into pUC19 (pUC19*ptipA*Δ) and sequenced. This reduced *ptipA* fragment (*ptipA*Δ) shown in the figure was mutagenized using the following primers (Δ, deleted base): M4, GTTTTCCCAGTCACGAC; RV, CAGGAAACAGCTATGAC; P1, CACGTGAGGΔGGCAGCGTGGACGGCGT; P2, CACGTGAGGΔΔGCAGCGTGGACGGCGT; P3, CACGTGAGGΔΔΔCAGCGTGGACGGCGTC; P4, CACGTGAGΔΔΔΔCAGCGTGGACGGCGTC; P5, TCCACGCTGCCΔΔΔCCTCACGTG; P6, TCCACGCTGCΔΔCCTCACGTGACG; P7, TCCACGCTGΔΔΔCCTCACGTGACG; P8, TCCACGCTGΔΔΔΔCTCACGTGACGT; P9, TTGCACCTCACGTΔACGTGAGGAGGCA; P10, TGCCTCCTCACGTΔACGTGAGGTGCAA. Upstream and downstream overlapping fragments containing the mutated sequence were generated in two separate reactions containing a mutant (P1−P10) and vector primer (RV, upstream; M4 downstream). The reactions employed the following primer pairs to generate deletions of 1−4 bases: Δ1, P1/M4 and P4/RV; Δ1′, P9/M4 and P10/RV; Δ2, P2/M4 and P6/RV, Δ3, P3/M4 and P7/RV; Δ4, P5/M4 and P8/RV. These mutated *ptipA* fragments were fused as a single fragment in a PCR reaction using primers RV and M4, cleaved with *Eco*RI and *Hin*dIII, inserted into pUC19, sequenced, and finally cloned into pIJ486::*ermE* (as a *Hin*dIII/*Eco*RI fragment).

Amino acid sequence homology puts TipAL in the MerR/SoxR/BmrR family of transcriptional regulatory proteins (*5*, *6*). An unusual feature of these proteins is that they bind between RNAP recognition hexamers centered around the nucleotide positions −10 and −35 upstream of the transcriptional initiation site. Members of this family, most of which have not yet been fully characterized, can be identified by their conserved N-terminal helix-turn-helix DNA binding motif of about 20 amino acids (*7*, *8*). In the case of MerR, the 30 amino acids that follow this motif affect the ability of the protein to interact with RNAP (*9*) either as a repressor or an activator (*10*). Dimerization requires a predicted helical domain including residues 80−128 (*11*). The diverse C-terminal domains of these proteins are involved in a variety of sensing functions. Mta, a multidrug resistance regulator recently reported in *Bacillus subtilis* (*12*), is the only member of the MerR family with homology to the extended C-terminal domain of TipAL.

The C-terminus of TipAL serves as a broad-spectrum thiopeptide recognition domain (*2*) that can be independently translated as TipAS. Thiostrepton binds covalently to TipAL and TipAS via one of its two C-terminal cysteine residues (*2*, *4*). In *S. lividans*, this covalent interaction apparently enables transcriptional activation at nanomolar concentrations of thiopeptide (*2*). Other transcriptional activators are recognized by different effector molecules: MerR by mercuric ion (*13*, *14*); SoxR by unknown oxidants (*15*); and Bmr and BltR by various antiseptics and drugs including rhodamine 6G and tetraphenylphosphonium chloride (TPP) (*16*). A structural basis for multidrug recognition has recently been revealed by the crystal structure of the C-terminal binding domain of BmrR complexed with TPP (*17*). Structural changes may mediate crosstalk between the N- and C-terminal domains that coordinates promoter, ligand, and RNAP interactions. This has been inferred from studies on Mta demonstrating that deletion of its C-terminal domain enables it to promote transcription in the absence of ligand (*12*).

Under noninducing conditions, MerR binds to the promoter and enhances RNAP binding (*18*, *19*). Binding of MerR (*8*) and SoxR (*20*) to their promoters is not enhanced by ligand interactions. In contrast, gel mobility shift assays suggested that thiostrepton enhanced TipAL binding to its promoter fragment, albeit at large protein/DNA molar ratios (*3*). These experiments do not however reveal discrete protein−DNA bands, which could reflect the instability of DNA−protein complexes during gel electrophoresis (*21*) or because the linear DNA fragments used in the assay do not possess the superhelical structure required for binding.

Upon activation, MerR undergoes a change in conformation that promotes transcription by causing the promoter to bend and twist (*3*, *8*, *22*, *23*) leading to open complex formation (*18*). This apparently compensates for the abnormally large nucleotide spacing between the −10 and −35 promoter recognition motifs. MerR- and SoxR-independent activation of their respective promoters can be achieved by single nucleotide deletions within this region (*24*, *25*). Corresponding mechanistic studies of other MerR/SoxR-related transcriptional activators have not yet been carried out.

To compare TipAL with other members of this family, binding events between regulator, RNAP and DNA need to be carefully monitored. An attractive route to obtaining this information is optical waveguide lightmode spectroscopy (OWLS), a relatively new technique which allows events at the solid/liquid interface to be probed noninvasively with good time resolution and excellent sensitivity (currently about 10^{-16} mol of protein/mm^2) (*26*). It has recently been successfully exploited to study the dynamics of restriction enzymes binding to DNA (*27*), many problems in the adsorption of proteins to solid surfaces (*28*), and the binding of antibodies and other ligands to membrane-anchored receptors (*26*, *29*). A further advantage of the method is that it permits determination of the absolute number of bound proteins per unit area of surface without ad hoc assumptions. Double stranded covalently closed circular superhelical plasmids containing *ptipA* were immobilized at a planar optical waveguide for measurement of the association and dissociation of the TipA proteins and RNAP under controlled hydrodynamic conditions. These studies, along with analytical ultracentrifugation (AU), circular dichroism (CD), and genetic analyses provided a model of thiostrepton-induced transcriptional activation.

MATERIALS AND METHODS

DNA and Plasmids. A 143-bp fragment containing *ptipA* was cloned into pUC19 to provide a double stranded closed circular plasmid for the DNA binding experiments [pAK113 (*1*)]. The plasmids were isolated from *Escherichia coli* W3110 cells grown at 37 °C in LB broth containing 100 μg/mL ampicillin using a Qiagen plasmid purification kit. The isolated plasmids were precipitated using cold 2-pro-

panol or ethanol (*30*) and resuspended in MA buffer (50 mM Tris-HCl, pH 8.0, 1 mM EDTA pH 8.0, and 100 mM NaCl). The plasmid, pIJ486*ermE*, was constructed by subcloning the erythromycin resistance gene, *ermE*, from pIJ4026 (provided by M. Bibb) into the *Kpn*I site of pIJ486 (*31*). The plasmid, pIJ486, has the thiostrepton resistance gene as its only selectable marker. The *ermE* gene allowed for selection of the promoter probe vector with erythromycin (flooding R2YE plates with 1 mL of 200 μg/mL erythromycin solution or NE plates containing 200 μg/mL erythromycin), thus avoiding induction of *ptipA*.

Proteins. TipAS and TipAL were produced in *E. coli* and purified as described earlier (*4*). Protein concentrations were determined by ultraviolet absorption with an extinction coefficient ($\epsilon_{280nm} = 23\,000\ M^{-1}\ cm^{-1}$) derived from amino acid analysis. *S. coelicolor* J1980 (*32*) was grown in YEME medium containing 5 mM $MgCl_2$, 34% (w/v) sucrose (*33*), and 10 μg/mL hygromycin to early stationary phase.

Total RNAP was isolated using the method of Buttner and Brown (*34*) with one modification: after the polymin P extractions and subsequent ammonium sulfate precipitation, Heparin Sepharose chromatography was performed instead of the DNA cellulose chromatography. The sample was loaded onto a 25 mL Heparin Sepharose Cl-6B (Pharmacia) column equilibrated in TGED buffer [0.1 M Tris-HCl, pH 7.9, 5% (v/v) glycerol, 0.1 mM EDTA, 0.1 mM dithiothreitol] containing 0.15 M NaCl. The column was washed extensively with TGED containing 0.2 M NaCl and RNAP was step-eluted with TGED containing 1 M NaCl. The eluate was dialyzed in TGED to a final salt concentration of 0.1 M NaCl and then applied to an 8 mL Source 15Q column (Pharmacia) equilibrated with the same buffer. After a washing step with TGED containing 0.2 M NaCl, RNAP was eluted with a 80 mL linear gradient of TGED buffer containing 0.7 M NaCl. Fractions (1 mL) were collected and analyzed on a 10% Laemmli SDS−PAGE gel. Fractions containing RNAP were identified by their α and $\beta\beta'$ subunits stained with Coomassie Brilliant Blue. Fifty microliter of each fraction containing RNAP were combined to yield the RNAP mixed holoenzymes (50 μg) that were used in the subsequent experiments.

The program PROSITE (www.expasy.ch) was used to predict the secondary structure of TipAL protein. The program COIL (www.ch.embnet.org/software) was used to predict the presence of a coiled coil motif (*35*).

Analytical Ultracentrifugation. Proteins were suspended in a buffer containing 50 mM Tris pH 7.0 250 mM NaCl, 1 mM EDTA, 10% v/v glycerol, 10% v/v DMSO. Sedimentation velocity (SV) and sedimentation equilibrium (SE) experiments were done in a Beckman XLA Optima analytical ultracentrifuge equipped with absorption optics at 20 °C. SV runs were carried out at 56 000 rpm in a 12 mm double sector Epon cell. SE runs were performed in the same cell type. The conventional SE method was used (*36*) and the cells were not meniscus depleted. Hence, the protein concentrations throughout the cell did not deviate significantly from the specified midpoint values. For the SE runs, rotor speeds were adapted to the different masses of the various molecules. A floating baseline computer program that adjusted the baseline absorbance to obtain the best linear fit of ln A vs r^2 (where A is absorbance and r the radial distance) was used. The density ($\rho = 1.032\ g/cm^3$) and viscosity ($\eta = 1.25$ cP) of the solution (assumed to be the same as those of the pure solvent) were estimated using standard reference tables (*37*). The protein partial specific volume was assumed to be 0.73 cm^3/g ($\nu = 0.73\ cm^3/g$). The molecular mass M_r was determined from the sedimentation equilibrium runs according to ref *36*

$$M_r = (2k_BT/((1 - \nu\rho)\omega^2))\ (2.303\ d\ \log\ c/dr^2) \quad (1)$$

where ω is the rotor angular velocity, k_B is the Boltzmann constant, T is the temperature, c is the protein concentration, and r is the radial distance in the cell. The sedimentation coefficient S was determined from the sedimentation velocity runs using the equation

$$S = (1/\omega^2 r)\ dr/dt \quad (2)$$

The protein diffusion coefficient D could then be determined from the sedimentation equilibrium and sedimentation velocity data according to

$$D = RTS/M_r\ (1 - \nu\rho) \quad (3)$$

where R is the gas constant.

CD Spectroscopy. The TipA proteins and their corresponding complexes with thiostrepton were dialyzed extensively against 25 mM potassium phosphate (pH 6.0). The CD spectra were measured at 20 °C under a nitrogen atmosphere in a Jasco J720 spectropolarimeter and averaged over at least 10 scans. The spectra were measured using 1 nm resolution, 1.0 nm bandwidth, 20 mdeg sensitivity, 2 s response, and a scan speed of 20 nm/min. Background spectra of buffer with thiostrepton were recorded and subtracted from samples containing protein and thiostrepton.

Optical Waveguide Lightmode Spectroscopy (OWLS). Planar optical waveguides equipped with a grating coupler (either Type 1400 or Type 2400 from Artificial Sensing Instruments, Zurich) were precoated with a layer of polyallylamine as described previously (*38*). This is an excellent substrate for binding DNA that apparently allows it to retain its native conformation (*27*). Either pAK113 or pUC19 were immobilized in situ, i.e., while carrying out OWLS (see below), to determine the amount of DNA immobilized on the substrate. The DNA immobilization was carried out in a closed cuvette, with gentle intermittent agitation. The rates of binding of both pUC19 and pAK113 plasmids were similar, as expected since pAK113 was derived from pUC19 (2686 bp) by the addition of a 143-bp fragment containing *ptipA*. The plasmid, pUC19, served as a nonspecific (i.e., not base specific) DNA control. Both plasmids were prepared in the same manner from the same host. The buffer used was 20 mM sodium phosphate at pH 7.0, 1 mM DTT, and 5% glycerol.

To measure the optical waveguide lightmode spectrum, the diffraction grating was incorporated into the waveguide to enable the excitation of the different peaks in the spectrum by varying the angle of incidence of an external light beam (wavelength = 632.8 nm) falling on the grating. The waveguide-cuvette assembly was mounted in an IOS-1 integrated optical scanner (Artificial Sensing Instruments, Zurich) that incorporated a precision goniometer measuring the angles corresponding to the spectral peaks with microradian precision (*39*). The entire spectrum was recorded

repeatedly in order to obtain kinetic data. The amount of adsorbed DNA and protein is calculated from the peak positions via the mode equations (*26*, *27*, *29*) using assumed refractive index increments of 0.26 and 0.18 cm^3/g for DNA and protein, respectively.

After removal of the DNA solution and flooding with buffer until no DNA was eluted, proteins were introduced into a flow-through cuvette with the optical waveguide as one of its sides, at a wall shear rate (γ) of 8.0 s^{-1} at 20 °C. Protein flow was continued until the binding approached saturation. Buffer flow was then resumed and the dissociation kinetics measured. The DNA was regenerated by removing all associated proteins with a brief flux of 5 M NaCl.

To measure the binding of RNA polymerase to DNA to which TipAL was already bound, following attachment of TipAL. Since the rates of dissociation of specifically bound TipAL was much slower than the rate of RNAP binding, it was not necessary to add TipAL to the RNAP solution.

Our basic concept for protein−DNA interaction is based on an initial encounter of the protein with an arbitrary (non-base-specific) site on the DNA followed by linear migration of the protein along the DNA until a specific binding site is encountered (*27*). Hence, the nonspecific association is an essential precursor to specific association leading to much greater efficiency in finding the specific binding site (*40*).

Non-base-specific association and dissociation of TipA proteins to DNA were characterized by rate coefficients k_a and k_d, according to the equation

$$d\Gamma_n/dt = c_1 s k_a - \Gamma_n k_d \quad (4)$$

where Γ_n is the amount of nonspecifically bound protein, s is the number of possible nonspecific binding sites per unit area [i.e., total base pairs (*41*)], and c_1 is the near-surface concentration of dissolved protein, which is related to the bulk concentration c_b (*27*) according to

$$c_1 = (c_b D/\delta + \Gamma_n k_d)/(D/\delta + s k_a) \quad (5)$$

where D is the protein diffusion coefficient and δ is the thickness of the diffusion boundary layer (*42*):

$$\delta = 3\,(xD/2\gamma)^{1/3} \quad (6)$$

where $x = 3.5$ mm is the distance from the inlet of the cuvette to the center of the measuring zone. Equation 4 was numerically integrated and fitted to the experimental pUC19 binding data with k_a and k_d as free parameters. Since this number of bound proteins is far smaller than the number of nonspecific binding sites, s was taken to remain constant.

The base-specific binding process is characterized by a rate coefficient (k_s), determined with the help of an additional equation,

$$d\Gamma_s/dt = k_s \Gamma_n\,(1 - \Theta_s) - k_t \Gamma_s \quad (7)$$

where Γ_s is the amount of specifically bound protein, Θ_s the average occupancy of the recognition site, defined by

$$\Theta_s = (\Gamma_s/M_r)/(s/B) \quad (8)$$

where B (= 2823) is the ratio of nonspecific to specific binding sites (the target plasmid, pAK113, is 2823 bp long and includes one specific binding site for the TipAL dimer), and k_t is the rate constant for dissociation from the recognition site. Equation 4 must accordingly be modified to become

$$d\Gamma_n/dt = c_1 s k_a - \Gamma_n k_d - k_s \Gamma_n\,(1 - \Theta_s) \quad (9)$$

Equations 7 and 9 were numerically integrated and fitted to the pAK113 binding data (note that the sum $\Gamma_s + \Gamma_n$ is the quantity measured by OWLS) with k_a, k_d, k_s, and k_t as free parameters, and with k_a and k_d as a first estimate expected to be the same as those determined for pUC19.

Table 1: Sedimentation Velocity and Sedimentation Equilibrium Data of TipA proteins

sample	theoretical M_r (kDa)[a]	experimental M_r (kDa)	$S_{20,w}$	D/D_0 [b]
TipAS	16.9	16.8 ± 0.5	1.8 ± 0.15	1.0 ± 0.1
TipAS-thio	18.5	18.9 ± 1.0	2.0 ± 0.15	1.0 ± 0.1
TipAL	28.8	48 ± 3	3.4 ± 0.2	1.0 ± 0.1
TipAL-thio	30.5	54 ± 3	3.5 ± 0.2	0.9 ± 0.1

[a] Note that since the stoichiometry of the TipAL-thiostrepton complex is 1:1 (*4*), two thiostrepton molecules should be bound to the dimer. [b] Ratio of measured diffusion or friction coefficients to those of ideal spheres.

RESULTS

Analytical Ultracentrifugation. Sedimentation velocity data (Table 1) showed that TipAS (the C-terminal domain of TipAL) and TipAS-thiostrepton complexes were monomers. The diffusion coefficients calculated from eq 3 were equal within experimental uncertainty to the Stokes−Einstein estimates for a perfect sphere [$D = k_B T/(6\pi\eta r)$ where r is the protein radius estimated from $r = [3M_r\nu/(4\pi N_a)]^{1/3}$]. Hence, there was practically no difference in shape in TipAS upon thiostrepton binding. Sedimentation equilibrium experiments (Table 1) showed no evidence of dimer formation (within the concentration range 0.1−7 mg/mL).

In contrast to TipAS, the measured sedimentation equilibrium results of TipAL and TipAL-thiostrepton showed that even at the lowest concentration investigated (0.15 mg/mL), they were predominately present as dimeric proteins (Table 1). Figure 3 shows SE data for TipAL-thio at two dilutions. At least 80% of the protein was present as the dimer in both cases, which gave indistinguishable results, putting an upper limit of the dimerization coefficient of approximately 10^{-6} M^{-1}. The difference in the ratio of the experimentally determined friction coefficient to that of a perfect sphere implied that the thiostrepton bound form was slightly ovoid.

Circular Dichroism. The CD spectra of the TipA proteins (Figure 4) had minima at 222 and 209 nm and a maximum below 200 nm. They suggested that both proteins have limited stable secondary structure, with some evidence for α-helicity in TipAL. There was little change in spectra for the TipA proteins with and without thiostrepton in the near UV region up to 330 nm. This suggested that the regions of TipAS and TipAL near the aromatic amino acids, which have absorption band maxima in region of 270−300 nm, were unchanged upon binding to thiostrepton. Secondary structure predictions from sequence data using PROSITE also indicate that TipAS has fewer secondary structural domains than TipAL; TipAL contains putative helix-turn-helix domains

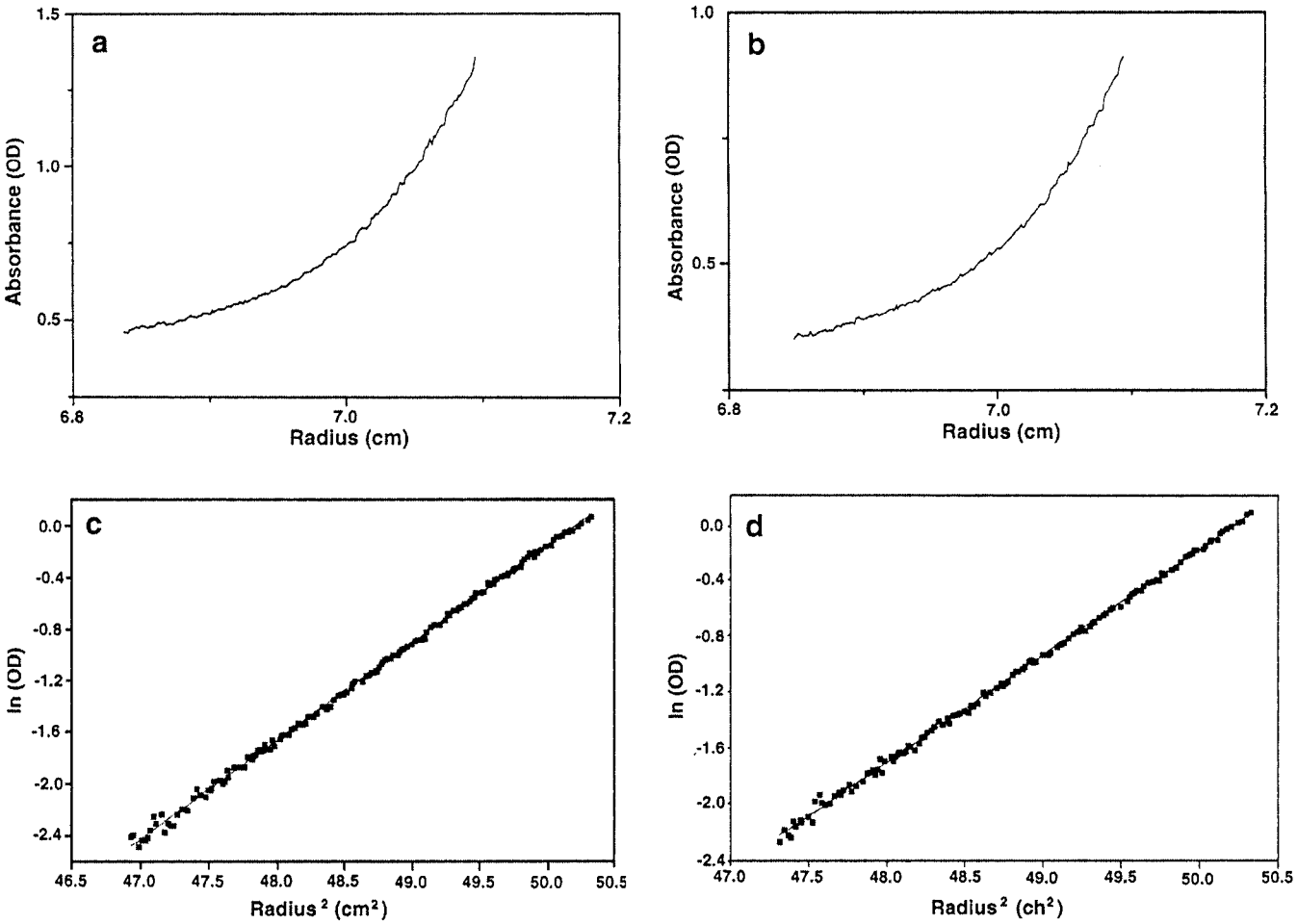

FIGURE 3: Sedimentation Equilibrium data for TipAS-thio. Sedimentation Equilibrium data for TipAS-thio panels a and b, raw data, panels c and d, data plotted according to eq 1. Panels a and c, protein concentration = 0.30 mg/cm^3; panels b and d, protein concentration = 0.15 mg/cm^3.

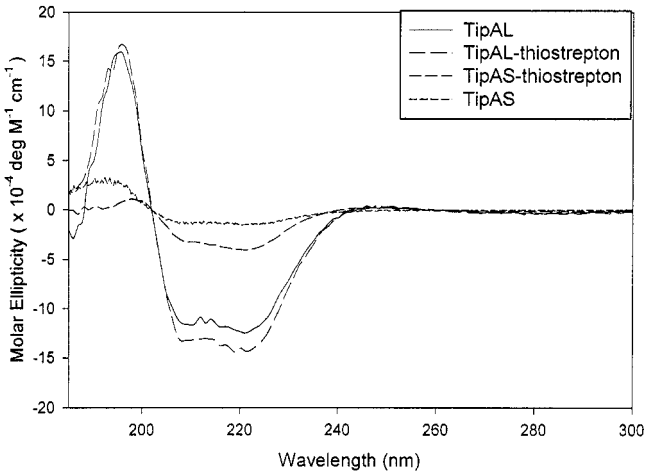

FIGURE 4: CD spectra of TipA proteins. CD spectra of TipAS, TipAS-thiostrepton, TipAL, and TipAL-thiostrepton were measured using 1 nm resolution, 1.0 nm bandwidth, 20 mdeg sensitivity, 2 s response, and a scan speed of 20 nm/min. TipAL had distinctly more α-helical content than TipAS, which increased upon binding to thiostrepton.

and a coiled coil (Figure 1) that would account for the additional α-helical character. After binding thiostrepton, both TipAS and TipAL slightly increased their alpha-helical contents. Since thiostrepton alone showed no significant CD features, this change was likely to be due to the protein, and would then indicate that the antibiotic induced a conformational change.

OWLS. OWLS was used to measure association and dissociation rates, and hence the binding constants, for both TipA protein dimers and RNAP with *ptipA*.

The affinity of TipAL for pAK113 (*ptipA* containing fragment cloned in pUC19) was much higher than that for pUC19 (Figure 5). Upon flooding with buffer, TipAL rapidly dissociated from pUC19 on a time scale comparable to that of the nonspecific association rate constant. However, the dissociation of TipAL from pAK113 was much slower, indicating specific binding between TipAL and *ptipA*. While thiostrepton had no measurable effect on the nonspecific binding of TipAL to pUC19 DNA, it increased the specific affinity of TipAL to pAK113 by more than 10-fold. The specific association rate constant increased slightly and the specific dissociation rate constant decreased upon thiostrepton binding (Table 2). The affinities of TipAS and TipAS-thiostrepton to both pUC19 and pAK113 were extremely weak (data not shown).

The affinities of *S. coelicolor* RNAP for *ptipA* and the TipAL and TipAL−thiostrepton complexes with DNA were similarly determined (Figure 6). *Streptomyces* RNAP preparations are mixtures of different holoenzymes containing an array of sigma subunits encoded by the *Streptomyces coelicolor* genome (http://www.sanger.ac.uk/Projects/S_coelicolor/). One or more components that may be present

Table 2: TipAL and RNAP Binding Parameters[a]

	nonspecific			specific		
	k_a (M^{-1} s^{-1}) (on rate)	k_d (s^{-1}) (off rate)	$K_d^{(ns)}$ (M)[a]	$k_{s/s}{}^{-1}$ (on rate)	$k_{t/s}{}^{-1}$ (off rate)[f]	$K_d^{(s)}$ (M)[b]
TipAL (pUC19)	100	0.021	2.1×10^{-4}	0.00	0.00	*c*
TipAL:thio (pUC19)	100	0.021	2.1×10^{-4}	0.00	0.00	*c*
TipAL (pAK113)	100	0.021	2.1×10^{-4}	0.27	0.0007	5.4×10^{-7}
TipAL:thio (pAK113)	100	0.021	2.1×10^{-4}	0.60	0.0001	3.5×10^{-8}
RNAP[d] (pUC19)	15	0.0012	8×10^{-5}	0.00	0.00	*c*
RNAP TipAL (pAK113)	26	0.01	4×10^{-4}	0.02	0.0007	1.4×10^{-5}
RNAP TipAL:thio (pAK113)	24	0.01	4×10^{-4}	0.02	<0.00001	$<2 \times 10^{-7}$

[a] Estimated errors are ± the last significant digit. [b] $K_d^{(ns)} = k_d/k_a$. [c] $K_d^{(s)} = k_d k_t/(k_a k_s)$. [d] Not defined. [e] These numbers refer to the sum of nonspecific and various specific interactions of a mixture of RNAP holoenzymes with pUC19. In the absence of TipAL, the kinetics of the interactions between RNAP and pUC19 or pAK113 were not significantly different. [f] All kinetic measurements were obtained from experiments repeated at least three times. In all the experiments in the presence of thiostrepton (TS), the off-rate was immeasurably small. Taking into account the average noise level of the measurements, this suggests that the off-rate with TS was at least 100 times smaller than that without TS.

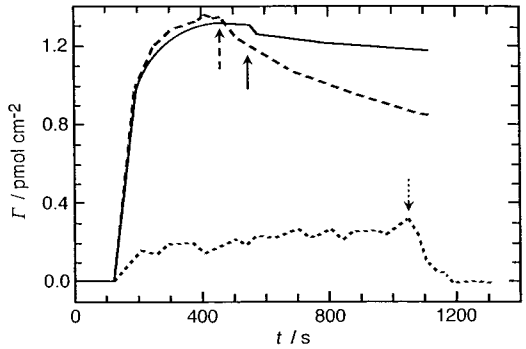

FIGURE 5: Kinetics of TipAL protein binding. The solid line represents TipAL-thio (at a bulk concentration c_b of 20 μg/cm^3) binding to pAK113 (0.21 nmol bp/cm^2); the dashed line represents TipAL ($c_b = 20$ μg/cm^3) binding to pAK113 (0.21 nmol bp/cm^2); the dotted line represents TipAL or TipAL-thio binding to pUC19. Samples began flowing at time $t = 0$, and the arrows mark the start of flooding with buffer. TipAL dissociated more rapidly from pAK113 than TipAL-thio. There was no difference between the association and dissociation of TipAL and TipAL-thio on pUC19.

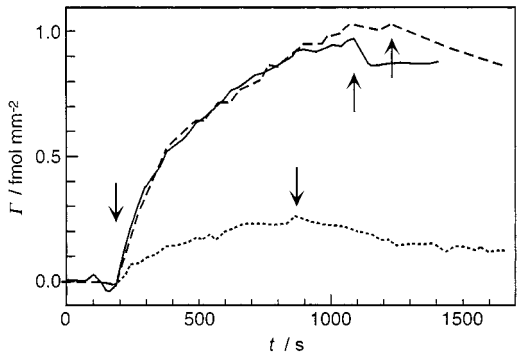

FIGURE 6: Kinetics of RNAP binding. The solid line shows RNA polymerase ($c_b = 35$ μg/cm^3) binding to TipAL-thio bound to pAK113 (0.11 nmol bp/cm^2); the dashed line shows RNA polymerase ($c_b = 45$ μg/cm^3) binding to TipAL bound to pAK113 (0.11 nmol of bp/cm^2); the dotted line shows RNA polymerase ($c_b = 40$ μg/cm^3) binding to pUC19 (0.21 nmol of bp/cm^2). Samples began flowing at time $t = 0$, and the arrows mark the start of flooding with buffer. RNAP dissociated from TipAL-thiostrepton bound to pAK113 more slowly than from TipAL bound to pAK113. RNA polymerase bound weakly to pUC19 alone. In all the experiments in the presence of thiostrepton (TS), the off-rate was immeasurably small. Taking into account the average noise level of the measurements, this suggests that the off-rate with TS was at least 100 times smaller than that without TS.

in the mixture can interact with the *lac* promoter (*43*) and possibly other promoters on pUC19. Consequently, the measured kinetics will represent an average from high and low affinity components. Equation 4 could be fitted to the RNAP binding data, yielding a weak affinity, slightly higher than the nonspecific interaction of TipAL with pUC19. *S. coelicolor* RNAP did not form stable complexes with *ptipA* (pAK113) unless TipAL was present. The RNAP affinity was enhanced more than a 100-fold by the presence of the TipAL-thiostrepton complex.

Genetic Analysis of the tipA Promoter. The *tipA* promoter fragment was subcloned to localize the region required for TipAL−thiostrepton-induced transcription. A fragment of 51 bp (*ptipA*Δ; Figure 2; from −48 to +2 relative to the transcriptional start site) was amplified by PCR and subcloned into a promoter probe vector pIJ486*ermE* (*31*). In the resulting plasmid, pAK100, a kanamycin resistance gene served as the reporter of promoter activity in either *S. lividans* 1326 or KT, a *S. lividans 1326* mutant in which the chromosomal *tipA* gene had been inactivated by site-directed mutagenesis (*2*). These strains were tested for thiostrepton-induced kanamycin resistance. pIJ486*ermE* containing *ptipA* allowed *S. lividans*, but not KT, to grow on NE agar (*44*) plates containing 40−400 μg/mL kanamycin in the presence of the inducer, thiostrepton. Neither of these strains grew on similar plates lacking thiostrepton.

This minimal *tipA* promoter was used to address the question of whether, as in MerR and SoxR promoters, inappropriate spacing of the −10 and −35 regions explains its lack of promoter activity in the absence of activator protein. In the case of MerR and SoxR, this defect could be offset by nucleotide deletions (*24*, *25*). The start site of *ptipA* has been mapped in vivo and in vitro (*1*, *3*). On the basis of these data, a series of adjacent 1, 2, 3, or 4 bp deletions were made in the corresponding region of *ptipA* (Δ1−Δ4, Figure 2). The location of these deletions had to be restricted to a region between the predicted −10 and −35 RNAP recognition hexamers and the minimal inverted repeat sequence within the TipAL binding site [mapped by DNase footprinting (*3*)]. Another unlinked 1-bp deletion further removed from the putative promoter hexamers (Δ1′), between the inverted repeat of the TipAL binding site was also constructed (Figure 2). These mutant promoters were tested for activity in pIJ486*ermE* using the same plate reporter gene assays. None of these promoter mutants provided induced or uninduced kanamycin resistance under these conditions in either *S. lividans* 1326 or KT.

DISCUSSION

We have applied a combination of different biophysical techniques including analytical ultracentrifugation, CD, and OWLS, to gain insights into the mechanism by which TipAL protein activates transcription from the *tipAL* promoter in response to thiostrepton. These techniques were used to analyze changes in dimerization, conformation, and specific DNA recognition leading to enhanced binding of RNAP to the promoter.

Dimerization. Analytical ultracentrifugation showed that TipAS and TipAS-thiostrepton were monomers and both TipAL and TipAL-thiostrepton were dimers within a wide range of concentration. Although TipAL may not be in a monomeric form at the submicromolar concentrations in the cell, DNase protection assays suggest that TipAL binds to ptipA as a dimer (*3*). This indicated that activation of TipAL by thiostrepton may not be mediated by dimerization. Instead, dimerization could an inherent property of the protein, presumably determined by its N-terminal 110 amino acid domain. TipAS, the C-terminal ligand-binding domain of TipAL (111−244), was not dimeric under our experimental conditions. Furthermore, secondary structure prediction programs suggested that the amino acid sequence 77−109 (Figure 1) had an α-helical structure that might dimerize via a putative coiled-coil interaction (*35*, *45*). A similar prediction (*46*), supported by experimental data (*11*), has been made for MerR. Hence the dimerization domain of TipAL resided in the N-terminal domain. However these results do not exclude the possibility that DNA binding could depend on a monomer−dimer equilibrium for TipAL.

Thiostrepton-Induced Changes in the Conformation of TipAL. CD spectral analysis indicated that thiostrepton induced changes in the α-helical content of the TipA proteins. The CD signal for TipAL at 209 and 222 nm was much greater than for TipAS, implying more α-helical structure within the N-terminal region (due to residues absent in TipAS). However, any quantitative interpretation of the α-helical content could be fraught with error since TipAL and TipAS could have differently sized domains. The differences between the TipAL and TipAL-thiostrepton secondary structures indicated conformational changes induced by thiostrepton binding. This small specific increase in α-helical structure suggests that thiostrepton does not act by denaturing a C-terminal domain, which then inhibits the N-terminal DNA binding activity. It is in accordance with the behavior of other transcriptional activators whose conformation also becomes more alpha-helical after ligand binding (*47*−*49*). In contrast, crystal structure analysis of a related multidrug sensor, BmrR (*17*), revealed that drug binding led to unfolding of a single α-helix. Further evidence for conformational changes comes from the observation that the specific on rate (rate of search, k_s) was doubled in the presence of thiostrepton (see discussion of OWLS results below).

TipAL-thio-Induced Changes in the Conformation of the tipA Promoter. TipAL might be similar to other MerR-type proteins that activate transcription after ligand interactions by untwisting or unwinding within the spacer region (*3*, *8*, *22*, *23*). In the case of MerR (*24*) and SoxR (*25*), the critical role of spacing can be demonstrated by the fact that nucleotide deletions within the −10 to −35 region allowed transcription in the absence of their respective activator proteins (*24*). However, in the case of *ptipA*, a series of comparable nucleotide deletions did not have such an effect. Gel retardation assays (M. Folcher and C. J. Thompson, unpublished data) showed that these mutant promoter fragments were able to bind TipAL-thio (with one exception, Δ1′). Nevertheless, instead of providing for constitutive expression in *S. lividans*, they had no detectable activity in the presence or absence of thiostrepton. Since MerR can function as a repressor, it was conceivable that this effect reflected a similar activity of TipAL on these mutant promoters. This was ruled out by the fact that these promoters were also inactive in a *tipAL* mutant strain (KT).

Thus, while the nonoptimal 19-bp spacing between putative RNAP recognition hexamers argues that TipAL-regulated promoters may act by unwinding the DNA between the −10 and −35 hexamers (*3*), genetic analyses similar to those that demonstrated the critical role of spacing for SoxR- and MerR-regulated promoters were inconclusive. We believe that the inactivation of deleted promoters results from unanticipated interactions between these bases and either RNAP or TipAL. Indeed, only bases outside the inverted repeat were targeted for deletion, to minimize their effects on TipAL binding. These bases were juxtaposed to the putative-10 hexamer and could possibly have inactivated the promoter. While none of these mutations were within the inverted repeat presumed to form the binding site for dimeric TipAL and the mutations did not prevent binding (M. Folcher and C. J. Thompson, unpublished data), deleted bases were within the zone of TipAL−DNA interaction as inferred from DNAse protection experiments (*3*). Furthermore, the recently determined structure of the BmrR−promoter complex shows that BmrR interacts with bases occupying corresponding positions. These bases participate in an extended conformational change in DNA structure catalyzed by ligand bound BmrR (*50*).

Thiostrepton-Induced Changes in TipAL Leading to Transcriptional Activation. TipAL bound only to the plasmid containing its own promoter fragment (pAK113). Whereas in the case of pUC19, rapid dissociation occurred upon flooding with buffer on a time scale comparable to that of association, dissociation from pAK113 was extremely slow, suggesting that it took place in the presence of a competing reaction, i.e., very strong association to the specific DNA binding site. According to the model developed earlier (*27*, *40*), the protein associates nonspecifically to the DNA and executes a random walk along the DNA until it dissociates. If the DNA contains a specific binding (recognition) sequence, then there is a finite probability that during the walk, the protein will encounter and bind to the recognition sequence, this process being characterized by the rate constant k_s which is directly related to the rate of walking along the DNA.

The increased affinity of TipAL in the presence of thiostrepton resulted primarily from a decrease in the rate of TipAL dissociation from the operator site. In the absence of thiostrepton, the affinity (K_d) of TipAL for its promoter was ca. 10^{-7} M, similar to that estimated from gel shift assays ($<10^{-7}$M) using renatured TipAL (*3*). This is lower than most values for other prokaryotic transcriptional regulatory proteins (10^{-8}−10^{-13}M) (*51*), especially MerR (promoter $P_T = 10^{-10}$ M) (*52*) and SoxR (*soxS* promoter = 10^{-10} M) (*15*).

The addition of thiostrepton increased the affinity to within this range.

TipAL dissociation appeared to be the rate-limiting step for RNAP release in the absence of thiostrepton. TipAL-thiostrepton increased the affinity of RNAP for *ptipA* more than 10-fold ($K_d < 10^{-7}$M), in agreement with a previous estimate for average RNAP−promoter closed complex formation in *E. coli* (K_d ca. $10^{-7}-10^{-8}$ M) (*53*). The observation that TipAL-thiostrepton/RNAP complex was more stably associated with the *tipA* promoter than TipAL-thiostrepton alone (Table 2) reflected stabilizing interactions within this transcriptional initiation complex. The measured stoichiometry of the RNAP binding specifically to the DNA (Figure 6) is 1:1 at the binding plateaus, which therefore corresponds to saturation of the binding. However, TipAL binding to DNA occurred in considerable excess with stoichiometry of monomeric protein:DNA being roughly 10:1. If the protein binds to the DNA as a dimer and considering possible uncertainties in the DNA and protein refractive index increment values, we are left with apparent excess specific binding of 1−2 TipAL dimers to the 143 bp insertion.

In contrast, MerR and SoxR transcriptional activity is not regulated by increased affinity to the promoter. Ligand binding has no effect on the affinity of SoxR for the SoxS promoter (*15*) and actually decreases the affinity of MerR for its promoter (*52*). This unanticipated feature of TipAL (and probably others, including BmrR (*16*)) showed that the mechanism by which it activates transcription is distinctively different from the well-characterized MerR/SoxR paradigm. Furthermore, TipAL differs from BmrR in that ligand binding resulted in opposite effects on overall protein α-helical structure.

These differing mechanisms of transcriptional activation nevertheless share a fundamentally important biological feature. Low concentrations of these transcriptional activators in the cytoplasm provide an ever-ready surveillance system that allows the organism to monitor and react swiftly to a progressively toxic environment. Within this family of transcriptional regulators, reaction can occur either by catalyzing transcription from preexisting RNAP promoter complexes [MerR (*54*)], or by increasing RNAP affinity for the promoter (*ptipA*), a function otherwise provided by specific RNAP subunits.

ACKNOWLEDGMENT

We thank Ariel Lustig for having carried out the analytical ultracentrifugation experiments; Marc Folcher with assistance with the TipA proteins and providing unpublished data; and Richard Brennan for critical comments and sharing of unpublished data.

REFERENCES

1. Murakami, T., Holt, T. G., and Thompson, C. J. (1989) *J. Bacteriol. 171*, 1459−1466.
2. Chiu, M. L., Folcher, M., Katoh, T., Puglia, A. M., Vohradsky, J., Yun, B.-S., Seto, H., and Thompson, C. J. (1999) *J. Biol. Chem. 274*, 20578−20586.
3. Holmes, D. J., Caso, J. L., and Thompson, C. J. (1993) *EMBO J. 12*, 3183−3191.
4. Chiu, M. L., Folcher, M., Griffin, P., Holt, T., Klatt, T., and Thompson, C. J. (1996) *Biochemistry 35*, 2332−2341.
5. Karlin, S., and Altschul, S. F. (1990) *Proc. Natl. Acad. Sci. U.S.A. 87*, 2264−2268.
6. Karlin, S., and Altschul, S. F. (1993) *Proc. Natl. Acad. Sci. U.S.A. 90*, 5873−5877.
7. Barrineau, P., Gilbert, P., Jackson, W. J., Jones, C. S., Summers, A. O., and Wisdom, S. (1984) *J. Mol. Appl. Genet. 2*, 601−619.
8. Summers, A. O. (1992) *J. Bacteriol. 174*, 3097−3101.
9. Caslake, L. F., Ashraf, S. I., and Summers, A. O. (1997) *J. Bacteriol. 179*, 1787−1795.
10. Comess, K. M., Shewchuk, L. M., Ivanetich, K., and Walsh, C. T. (1994) *Biochemistry 33*, 4175−4186.
11. Zeng, Q., Stalhandske, C., Anderson, M. C., Scott, R. A., and Summers, A. O. (1998) *Biochemistry 37*, 15885−15895.
12. Baranova, N. N., Danchin, A., and Neyfakh, A. (1999) *Mol. Microbiol. 31*, 1549−1559.
13. Helmann, J. D., Ballard, B. T., and Walsh, C. T. (1990) *Science 247*, 946−948.
14. Helmann, J. D., Shewchuk, L. M., and Walsh, C. T. (1990) *Adv. Inorg. Biochem. 8*, 33−61.
15. Hidalgo, E., and Demple, B. (1994) *EMBO J. 13*, 138−146.
16. Ahmed, M., Borsch, C. M., Taylor, S. S., Vazquez-Laslop, N., and Neyfakh, A. A. (1994) *J. Biol. Chem. 269*, 28506−28513.
17. Zheleznova, E. E., Markham, P. N., Neyfakh, A. A., and Brennan, R. G. (1999) *Cell 96*, 353−362.
18. Frantz, B., and O'Halloran, T. V. (1990) *Biochemistry 29*, 4747−4751.
19. Heltzel, A., Lee, I. W., Totis, P. A., and Summers, A. O. (1990) *Biochemistry 29*, 9572−95784.
20. Hidalgo, E., and Demple, B. (1997) in *Regulation of gene expression in Escherichia coli* (Lin, E. C. C., and Lynch, A. S., Eds.) pp 433−450, R. G. Landes, Co., Austin, TX.
21. Lane, D., Prentki, P., and Chandler, M. (1992) *Microbiol. Rev. 56*, 509−528.
22. Ansari, A. Z., Chael, M. L., and O'Halloran, T. V. (1992) *Nature 355*, 87−89.
23. Ansari, A. Z., Bradner, J. E., and O'Halloran, T. V. (1995) *Nature 374*, 371−375.
24. Parkhill, J., and Brown, N. (1990) *Nucleic Acids Res. 18*, 5157−5162.
25. Hidalgo, E., and Demple, B. (1997) *EMBO J. 16*, 1056−1065.
26. Ramsden, J. J., and Schneider, P. (1993) *Biochemistry 32*, 523−529.
27. Ramsden, J. J., and Dreier, J. (1996) *Biochemistry 35*, 3746−3753.
28. Ramsden, J., Roush, D., Gill, D., Kurrat, R., and Willson, R. (1995) *J. Am. Chem. Soc. 117*, 8511−8516.
29. Ramsden, J. J., and Wright, C. S. (1995) *Glycoconjugate J. 12*, 113−121.
30. Sambrook, J., Fritsch, E. F., and Maniatis, T. (1989) *Molecular Cloning. A Laboratory Manual*, 2nd ed., Cold Spring Harbor Laboratory Press, New York.
31. Ward, J. M., Janssen, G. R., Kieser, T., Bibb, M. J., Buttner, M. J., and Bibb, M. J. (1986) *Mol. Gen. Genet. 203*, 468−478.
32. Babcock, M. J., Buttner, M. J., Keler, C. H., Clarke, B. R., Morris, R. A., Lewis, C. G., and Brawner, M. E. (1997) *Gene 196*, 31−42.
33. Hopwood, D. A., Bibb, M. J., Chater, K. F., Kieser, T., Bruton, C. J., Kieser, H. M., Lydiate, D. J., Smith, C. P., Ward, J. M., and Schrempf, H. (1985) *Genetic Manipulation of Streptomyces. A Laboratory Manual*, The John Innes Foundation, Norwich, U.K.
34. Buttner, M. J., and Brown, N. L. (1985) *J. Mol. Biol. 185*, 177−188.
35. Lupas, A., Van Dyke, M., and Stock, J. (1991) *Science 252*, 1162−1164.
36. Chervenka, C. H. (1970) *A Manual of Methods for the Analytical Ultracentrifuge*, Beckman Instruments, Palo Alto.
37. Weast, R. (1981) *Handbook of Chemistry and Physics*, 62 ed., CRC Press, Boca Raton, FL.
38. Ramsden, J. J., Lvov, Y. M., and Decher, G. (1995) *Thin Solid Films 254*, 246−251.
39. Tiefenthaler, K. (1992) *Adv. Biosensors 2*, 261−289.
40. Ramsden, J. J. (2000) *Colloids Surf., A 173*, 237−249.

41. McGhee, J. D., and Hippel, P. H. v. (1974) *J. Mol. Biol. 86*, 469−489.
42. Levich, B. (1947) *Discuss. Faraday Soc. 1*, 37−43.
43. Jaurin, B., and Cohen, S. N. (1984) *Gene 28*, 83−91.
44. Murakami, T., Anzai, H., Imai, S., Satoh, A., Nagaoka, K., and Thompson, C. J. (1986) *Mol. Gen. Genet. 205*, 42−50.
45. Berger, D., Wilson, D. B., Wolf, E., Tonchev, T., Milla, M., and Kim, P. S. (1995) *Proc. Natl. Acad. Sci. U.S.A. 92*, 8259−8263.
46. Caguiat, J. J., Watson, A. L., and Summers, A. O. (1999) *J. Bacteriol. 181*, 3462−3471.
47. O'Neill, K. T., Schuman, J. D., Ampe, C., and DeGrado, W. F. (1991) *Biochemistry 30*, 9030−9034.
48. Uesugi, M., Nyaguile, O., Lu, H., Levine, A. J., and Verdine, G. L. (1997) *Science 277*, 1310−1313.
49. Ferre-D'Amare, Pognonec, P., Roeder, R. G., and Burley, S. K. (1994) *EMBO J. 13*, 180−189.
50. Heldwein, E. E., and Brennan, R. G. (2001) *Nature 409*, 378−382.
51. Ramesh, V., De, A., and Nagaraja, V. (1994) *Protein Eng. 7*, 1053−1057.
52. Parkhill, J., Ansari, A. Z., Wright, J. G., Brown, N. L., and O'Halloran, T. V. (1993) *EMBO J. 12*, 413−421.
53. McClure, W. R. (1985) *Annu. Rev. Biochem. 54*, 171−204.
54. Ralston, D. M., and O'Halloran, T. V. (1990) *Proc. Natl. Acad. Sci. U.S.A. 87*, 3846−3850.

BI010328K